Mottarlini Francesca (Orcid ID: 0000-0001-8172-1384)
Targa Giorgia (Orcid ID: 0000-0003-2933-2677)
Fumagalli Fabio (Orcid ID: 0000-0002-8814-7706)
Caffino Lucia (Orcid ID: 0000-0001-8045-3146)

Cortical reorganization of the glutamate synapse in the activity-based anorexia rat model: impact on cognition

Francesca Mottarlini, PhD, Giorgia Targa, M.Sc., Giorgia Bottan, M.Sc., Benedetta Tarenzi, M.Sc., Fabio Fumagalli, Professor, and Lucia Caffino, Professor*

Department of Pharmacological and Biomolecular Sciences, Università degli Studi di Milano, Via Balzaretti 9, 20133 Milano, Italy.

*Corresponding author: *Lucia Caffino*, Department of Pharmacological and Biomolecular Sciences, Università degli Studi di Milano, Via Balzaretti 9, 20133 Milano, Italy Phone 39-2-50318298

E-mail: Lucia.Caffino@unimi.it

ORCID ID: 0000-0001-8045-3146

Running title: Anorexia alters cortical dendritic spines and cognition

Keywords: adolescence, prefrontal cortex, glutamatergic synapse, activity-based anorexia, dendritic spine, cognition

Abstract

Patients suffering from anorexia nervosa (AN) display altered neural activity, morphological and functional connectivity in the fronto-striatal circuit. In addition, hypoglutamatergic transmission and aberrant excitability of the medial prefrontal cortex (mPFC) observed in AN patients might underpin cognitive deficits that fuel the vicious cycle of dieting behavior. To provide a molecular mechanism, we employed the activity-based anorexia (ABA) rat model, which combines the two hallmarks of AN (i.e. caloric restriction and intense physical exercise), to evaluate structural remodeling together with alterations in the glutamatergic signaling in the mPFC and their impact on temporal memory, as measured by the temporal order object recognition (TOOR) test.

Our data indicate that the combination of caloric restriction and intense physical exercise altered the homeostasis of the glutamate synapse and reduced spine density in the mPFC. These events, paralleled by an impairment in recency discrimination in the TOOR test, are associated with the ABA endophenotype. Of note, after a 7-day recovery period, body weight was recovered and the mPFC structure normalized but ABA rats still exhibited reduced post-synaptic stability of AMPA and NMDA glutamate receptors associated with cognitive dysfunction.

Taken together, these data suggest that the combination of reduced food intake and hyperactivity affects the homeostasis of the excitatory synapse in the mPFC contributing to maintain the aberrant behaviors observed in AN patients. Our findings, by identifying novel potential targets of AN, may contribute to more effectively direct the therapeutic interventions to ameliorate, at least, the cognitive effects of this psychopathology.

Abbreviations

ABA: activity-based anorexia (voluntary running activity in a mechanical wheel + food restriction)

AMPA receptor: α-amino-3-hydroxy-5-methyl-4-isoxazolepropionic acid receptor

AN: anorexia nervosa

ANOVA: analysis of variance

CTRL: control (sedentary + food *ad libitum*)

DSM-5: diagnostic and statistical manual of mental disorder (5th edition)

EXE: exercise (voluntary running activity in a mechanical wheel + food *ad libitum*)

EU: European Union

F-Actin: filamentous actin protein (RRID: AB_302794)

FR: food-restricted (sedentary + food restriction)

GluA1/A2: glutamate AMPA receptor 1/2 subunit (RRID: AB_641040, AB_10622024)

GluN1/2A/2B: glutamate NMDA receptor 1/2A/2B subunit (RRID: AB_1904067, AB_2112295, AB_2798506)

HEPES: 4-(2-hydroxyethyl)-1-piperazineethanesulfonic acid

mPFC: medial prefrontal cortex

NIH: National Institutes of Health

NMDA receptor: N-methyl-D-aspartate receptor

OD: optic density

PMSF: phenylmethylsulfonyl fluoride

PND: post-natal day

PSD: postsynaptic density

PSD95: postsynaptic density protein 95 (RRID: AB_561221)

RRID: Research Resource Identifier

SD: standard deviation

TIF: Triton X-100 insoluble fraction (or postsynaptic density)

TOOR: temporal order object recognition

SAP97: synapse associated protein 97; AMPA receptor scaffolding protein (RRID: AB_2091910)

SAP102: synapse associated protein 102; NMDA receptor scaffolding protein (RRID: AB_2799325)

1. Introduction

Anorexia nervosa (AN) is a serious psychiatric disorder affecting females tenfold more than males (DSM-V 2013; Micali & Dahlgren 2016) primarily during adolescence (Nagl *et al.* 2016; Schmidt *et al.* 2017), a period of life extremely vulnerable to external stimuli. AN begins with a self-inflicted restrictive diet to lose weight combined with intense physical activity and it progresses towards an out-of-control spiral, in which the positive experience of control over food intake and the severe exercise is indeed extremely rewarding for the patient, reinforcing the dieting behavior. Owing to the vulnerability of adolescents to unstable temperament, fragile personality traits and the imposed socio-cultural model of the body, many teenagers start developing anorexic behaviors because they perceive themselves as overweight, even though they are malnourished and emaciated: accordingly, food avoidance, weight control, and physical activity become real obsessions. Although AN shows the highest rate of mortality among all mental disorders (Sullivan 1995; Arcelus *et al.* 2011; Klump 2013) and despite growing knowledge about disease symptomatology, the etiopathogenesis of the disease remains unclear, treatment is challenging and often hampered by high relapse (Himmerich *et al.* 2020; Berends *et al.* 2016).

At the neurobiological level, it has been suggested that the driving force of such abnormal behavior might be represented by an altered balance between reward and inhibition mechanisms (Zink & Weinberger 2010; Wierenga *et al.* 2014), the latter being normally triggered by the medial prefrontal cortex (mPFC) that is immature and still growing during adolescence (Sakurai & Gamo 2019). Such dysfunctional mechanisms, combined with emotional dysregulation, may lead to a distorted response to ient stimuli, i.e. food, fueling the maintenance of the anorexic phenotype (Kaye 2008; Hildebrandt *et al.* 2015). Interestingly, anorexic patients are characterized by working memory and cognitive impairments (Nikendei *et al.* 2011; Fuglset 2019; Reville *et al.* 2016), presumably as a consequence of alterations in thalamo-frontal connectivity (Biezonski *et al.* 2016). Furthermore, several studies employing neuroimaging techniques revealed altered neural and metabolic activity, and morphological and functional connectivity in the brain of AN patients, specifically in regions related to fronto-striatal and limbic circuits (Friederich *et al.* 2013; Lipsman *et al.* 2015; Monteleone *et al.* 2018); also, brain volume changes have been observed in frontal, temporal, and visual cortices (Amianto *et al.* 2013; Cowdrey *et al.* 2014; Yau *et al.* 2013). Evidence exists, in both AN patients and animal models, that maladaptive reorganization of the mesocorticolimbic structures may represent the neurobiological underpinning of the motivational mechanisms underlying AN phenotype (Foldi *et al.* 2017; Ho *et al.* 2016; Frank *et al.* 2018). In this scenario, it is possible to hypothesize that dysfunctions of glutamate homeostasis, which has been

proposed as a signal of altered processing of food reward (Mottarlini *et al.* 2020; Ohrmann *et al.* 2004; Murray & Holton 2021), may contribute to the anorexic phenotype. This possibility is supported by a recent pilot study at 7 Tesla, in which Godlewska and coworkers found that glutamate levels were diminished in the occipital cortex of AN patients, anterior cingulate cortex and putamen, whereas the ratio of glutamine to glutamate was significantly increased, suggesting a hypoglutamatergic transmission in AN (Godlewska *et al.* 2017). Notably, activation of the mPFC is consistently altered in AN patients performing the Wisconsin Card Sorting Test (Sato *et al.* 2013) or challenged with a Go/NoGo task (Lock *et al.* 2011); besides, such patients also show aberrant excitability of the mPFC following different food-stimuli tests, an effect partially conserved even after a long period of recovery, highlighting an altered reward-related response to a pleasurable stimulus, pointing to dysfunctions in food information processing (Sanders *et al.* 2015; Ehrlich *et al.* 2015; Kullmann *et al.* 2014).

To this end, it is intriguing that dysregulation of mPFC activity, as observed in AN patients, is also found in a validated experimental model of AN (Schalla & Stengel 2019), the activity-based anorexia (ABA) rat model, in which the mPFC is hypometabolic as shown by micropositron emission tomography (van Kuyck *et al.* 2007). Interestingly, ABA rodents and AN patients show behavioral, hormonal, anatomical and neurochemical similarities, highlighting the translational relevance of this model (Barbarich-Marsteller *et al.* 2013; Gutierrez 2013). Of note, previous studies using this model demonstrated that enlargement of GABAergic terminal contacts onto pyramidal neurons of the mPFC in adolescent female mice facilitates response selection suppressing food restriction-evoked hyperactivity (Chen *et al.* 2016). Moreover, in the ABA rat model, significant alterations in dendritic branching and synaptic contacts in the mPFC and hippocampus were observed in both ABA and in lone food-restricted rats (Chowdhury *et al.* 2014; Aoki *et al.* 2017), suggesting that structural changes likely take place in AN. Taken together, these data suggest that a malnutrition-induced impairment of brain morphology and connectivity may have a role in the behavioral phenotype of AN; however, little is known about the molecular underpinning(s) that might mediate the development of pathological weight loss and aspects of cognitive dysfunction in this disorder.

Thus, based on the above-mentioned evidence, the main goal of this study was to evaluate whether the combination of food restriction and intense exercise, culprits of AN, induces cortical structural remodeling together with alterations in the glutamatergic signaling leading, in turn, to dysfunction in the recency discrimination that might trigger the motivational loop underlying AN (Lamanna *et al.* 2019). To this end, we set up the ABA rat model according to the literature (Carrera *et al.* 2014; Scherma *et al.* 2019; Schalla & Stengel 2019). Using such an animal model of AN, we investigated dendritic spine morphology and density as well as the expression of markers of the

glutamate synapse in the mPFC. Female adolescent rats were exposed to the combination of food restriction and intense exercise during adolescence and then sacrificed at two different time points: 1) during the acute phase of the pathology, once they achieved the anorexic phenotype (represented by the 25% of weight loss and wheel activity increasing over days), to evaluate the anorexic-induced alterations and 2) after a period of body weight recovery, with no more food deprivation or access to wheel activity, to identify possible molecular scars that might persist in the brain even when the body weight is restored. Then, to investigate whether the induction of the anorexic phenotype might cause cortical cognitive impairments, as observed in humans, we exposed another cohort of female adolescent ABA rats to a specific behavioral task, the temporal order object recognition (TOOR) test, at both experimental time points.

2. Material and Methods

2.1 Subjects

Female inbred Sprague-Dawley rats (RRID: RGD_734476) were obtained from Charles River (Calco, Italy) at postnatal day (PND)24, during adolescence, maintained under standard conditions of temperature (21±1 °C) and humidity (50-60%), and under a reversed 12 h light/dark cycle (lights on/off: 10.30 pm/10.30 am). A maximum of two female siblings was taken from each litter in order to reduce "litter effects" (Chapman & Stern 1978). Then the animals were arbitrarily divided into the experimental groups by chance with no regard to the will of the researcher. No randomization was performed to allocate subjects in the study. Animals were fed with standard rat chow (ssniff Spezialdiäten GmbH, Soest, Germany) with tap water *ad libitum.*

All animal procedures were conducted at the Department of Pharmacological and Biomolecular Sciences (University of Milan), and carried out in accordance with the principles set out in the following laws, regulations, and policies governing the care and use of laboratory animals: Italian Governing Law (D.lgs 26/2014; Authorization n.19/2008-A issued March 6, 2008, by Ministry of Health); the NIH Guide for the Care and Use of Laboratory Animals (2011 edition) (Paxinos & Watson 2013) and EU directives and guidelines (EEC Council Directive 2010/63/UE). Authorization for animal use has been obtained from the Italian Ministry of Health (#898-2016-PR). All efforts were made to minimize animal suffering and to keep the lowest number of animals used: for ethical reasons, activity-based anorexia (ABA) rats were not allowed to lose more than 25% of their initial body weight. The experiments have been reported in compliance with the ARRIVE guidelines. The present study was not pre-registered.

2.2 Experimental Design and Procedures

Figure 1a shows a schematic representation of the experimental paradigm. Briefly, upon arrival at PND 24, rats were group-housed and left undisturbed in their home cages to habituate to the light cycle for 11 days prior to the beginning of the experimental procedures. At PND35 animals were individually housed in transparent cages lined with dust-free woodchips, in the same room without any auditory isolation, and arbitrarily subdivided into four groups: [1] *control* (CTRL) group: sedentary + food *ad libitum*; [2] *food-restricted* (FR) group: sedentary + food restriction (food access limited for 2h/day), [3] *exercise* (EXE) group: voluntary running activity in a mechanical wheel (activity wheel BIO-ACTIVW-R cage, Bioseb, France) + food *ad libitum*, and [4] *activity-based anorexia* (ABA) group: voluntary running activity in a mechanical wheel + food restriction (food limitation for 2h/day). After three days of

acclimation period to the new housing condition, the food restriction period started at PND38, FR and ABA rats were subjected to caloric restriction with food limited for 2 h/day from 10.30 to 12.30 a.m., and during the 2 h of food access the wheel was blocked to prevent the rats preferring to run rather than to eat. At PND42, half of the animals/group were sacrificed, while the remaining animals were preserved sedentary with food ad libitum for 7 days until PND49 to allow body weight recovery.

Separate sets of rats were used to set up the protocol and for behavioral and molecular analysis *(Experiment 1: n=48; 4 experimental groups for each time point: CTRL n=6, FR n=6, EXE n=6, ABA n=6),* for spine density and morphological studies *(Experiment 2: n=16; 2 experimental groups for each time point: CTRL n=4, ABA n=4),* and for temporal memory performance evaluation *(Experiment 3; n =40; 2 experimental groups for each time point: CTRL n=10, ABA n=10, 2 animals for time point were excluded as described in paragraph 2.6*) (for a breakdown chart, including number of animals per experimental group per each experiment performed, number of excluded animals and time-point of exclusion, please refer to Supplementary figure 1).

After decapitation, the medial prefrontal cortex (mPFC, defined as Cg1, Cg3, and IL subregions) corresponding to plates 5–9 of the atlas of Paxinos and Watson, 2013 was immediately dissected from 2-mm-thick slices, frozen on dry ice, and stored at −80°C.

2.3 Measurements

Body weight, food intake and wheel running activity were assessed per each animal daily between 09.30 and 10.30 a.m., before the dark shift. Food intake was calculated as grams of food given at the beginning the 2h of food access – grams weighed at the end of the 2h. Running wheel data were recorded, via a monitoring software (BIO-ACTIVW-SOFT), at 30 minutes intervals for the entire duration of the experiments.

2.4 Dendritic spine labeling and morphological classification

Consequent to the ABA procedure, at PND42 and PND49 (CTRL, ABA: 4 rats/group, experiment 2), neuronal labeling and morphological classification of dendritic spines in layer V of the mPFC, primarily formed by glutamatergic pyramidal neurons, were carried out using a lipophilic membrane tracer as previously published (Caffino *et al.* 2015). The number of neurons used for quantification is at least 28 for each experimental group (from each neuron, a different number of dendritic segments was analyzed); neurons analyzed were belonging to 8 hemispheres per group. The average dendritic length analyzed is 130 μm, and the length of the total dendrites analyzed was of 4000 μm for each experimental group.

Analysis of dendritic spine morphology was performed with Fiji software released by ImageJ software; for each protrusion, we measured spine length, head, and neck width, which was used to classify dendritic spines into three categories (thin, stubby, and mushroom) (Harris *et al.* 1992; Gardoni *et al.* 2012). An operator who was 'blind' to the experimental conditions performed both image acquisition and quantification.

2.5 Preparation of Protein Extracts and Western Blot Analyses

Proteins from mPFC were extracted in cold 0.32 M sucrose buffer pH 7.4 containing 1 mM HEPES, 1 mM $MgCl_2$, 1 mM $NaHCO_3$ and 0.1 mM PMSF, in presence of commercial cocktails of protease (Roche, Monza, Italy) and phosphatase (Sigma-Aldrich, Milan, Italy) as previously described (Caffino *et al.* 2020a), quantified according to the Bradford Protein Assay procedure (Bio-Rad, Milan, Italy), using bovine serum albumin as calibration standard, and stored at −20 °C.

Western blots were run using sodium dodecyl sulfate-8% polyacrylamide gel under reducing conditions as previously described (Caffino *et al.* 2017) on the whole homogenate and on the TIF fraction, Triton X-100 insoluble fraction or postsynaptic density (PSD) and then electrophoretically transferred (dry transfer) onto nitrocellulose membranes (GE Healthcare, Milan, Italy). The strips of nitrocellulose membrane close to the molecular weights at which the bands of the protein of interest were expected were cut from the entire squared blot (full areas) as suggested by their specific molecular weight and the information present in the datasheet of the antibody. Blots were blocked one hour at room temperature with I-Block solution (Life Technologies Italia, Italy) in TBS + 0.1% Tween-20 buffer and washed with S + 0.1% Tween-20 buffer. The conditions of the primary and secondary antibodies were reported in table 1.

Results were standardized to α-tubulin control protein that was detected by evaluating the band density at 50 kDa (1:20.000, Sigma, RRID: AB_477593). Immunocomplexes were visualized by chemiluminescence using the Chemidoc MP Imaging System (Bio-Rad Laboratories) and example of full-size original cropped immunoblots are presented in the supplementary figures (S5-S10). Gels were run two times each, and the results represent the average from two different runs. We used a correction factor to average the different gels: correction factor gel B = average of (OD protein of interest/OD α-tubulin for each sample loaded in gel A)/(OD protein of interest/OD α-tubulin for the same sample loaded in gel B) (Caffino *et al.* 2020b).

2.6 Temporal Order Object Recognition (TOOR) test

The experimental apparatus used for the TOOR, a cognitive demanding test chosen to evaluate temporal memory abilities driven primarily by mPFC, was a black open-field box (60x60x60 cm) made of Plexiglas. This task (experiment 3, Fig 5a) comprised two sample phases (5 min duration each, with a delay in between of 1 h) and one test phase (5 min duration, performed 3 h after sample phase 2). During the test, a single third copy of the objects from sample phase 1 and a single third copy of the objects from sample phase 2 were used. Both objects and their placement were counterbalanced. Exploratory behavior was defined as the animal directing its nose toward the object at <2 cm of distance and sniffing, or snout directed to the object. Any subjects that failed to complete a minimum of 15 s exploration in the sample phase or 10 s of exploration in the test phase were excluded from the analysis (total exploration time is presented as supplementary figure S4 panel b). A total of 4 adolescent animals were removed from the study because they failed to successfully explore the objects (more than 10 s) during the sample phase 1 or 2. Exploration time was taken by two independent investigators, blind to the experimental design.

During the test phase, we measured two different indexes: 1) the recency discrimination index, that was calculated as the difference in time spent by each animal exploring the object from sample phase 1 compared with the object from sample phase 2 divided by the total time spent exploring both objects in the test period; and 2) the recognition index, that was considered as a measure of approach to both objects, was calculated as the time spent investigating the object presented in phase 1 or the object presented in phase 2 relative to the total object investigation time.

2.7 Data analysis and statistics

Data were collected in individual animals (independent determinations) and are presented as means and standard errors. Body weight, food intake and wheel activity were analyzed by two-way analysis of variance (ANOVA) with repeated measures followed by Bonferroni's multiple comparisons test. Samples sizes were calculated using the software G*power 3.1.9.2 (http://gpower.hhu.de/) with an effect size=0.4 (large, behavioral analysis), 0.25 (medium, molecular analysis), α error probability=0.05, power=0.8. The Kolmogorov–Smirnov test was employed to determine normality of residuals, and no significant variance in homogeneity was found.

Molecular changes were analyzed initially by a three-way (analysis of variance) ANOVA to investigate manipulations- and time-related differences, incorporating the following variables: food availability (food *ad libitum* vs food restriction), physical activity (sedentary vs exercise) and time of sacrifice (PND42 acute phase vs PND49 after recovery). As dictated by the relevant interaction terms, low-order ANOVAs

were used to determine manipulation effects and interactions followed by Bonferroni's multiple comparisons test to characterize differences between groups.

Morphological changes were analyzed by two-way ANOVA, with manipulation (control vs ABA) and time of sacrifice (PND42 acute phase vs PND49 after recovery) as independent variables. When dictated by relevant interaction terms, Bonferroni's multiple comparisons test was used to characterize differences among individual groups of rats.

The recency discrimination index measured in the TOOR test was analyzed using a two-way ANOVA, manipulation (control vs ABA) and time of sacrifice (PND42 acute phase vs PND49 after weight recovery). The recognition index measured in the TOOR test was analyzed using a three-way ANOVA, manipulation (control vs ABA), object (object phase 1 vs object phase 2) and time of sacrifice (PND42 acute phase vs PND49 after weight recovery). Fisher's least significant difference (LSD) test was used to characterize differences among individual groups of rats. However, when no interaction between manipulation and time of sacrifice was observed, only the main effects were reported. Detailed statistics, such as F and p values of independent variables of two-way or three-way ANOVA, were reported in the supplementary tables (S1, S2, S3, S4).

Pearson's product-moment coefficients were calculated to study potential correlations between behavioral outcomes induced by the ABA procedure, related to the wheel-running activity and body weight, molecular changes observed in the postsynaptic density of the PFC of ABA rodents and recency discrimination index measured in the TOOR test.

Subjects were eliminated from the final dataset if their data deviated from the mean by 2 SDs. Prism 2.1 (GraphPad Software, Prism v8.2.1, San Diego, CA, USA) was used to analyze all the data. Significance for all tests was assumed at $p < 0.05$.

3. Results

During the first experimental days (PND31-PND38), the average body weight of all four groups (CTRL; FR; EXE; ABA) increased constantly, with no significant differences resulting from wheel access (PND35-PND38). After 24 hours of food restriction, ABA and FR average body weight was significantly reduced compared to CTRL and EXE weight, this divergence was constantly increased over experimental days. Interestingly, at PND 42, ABA rats reduced body weight significantly more than FR rats (Fig 1b), despite similar food intake (Fig 1c). Refeeding schedule (food *ad libitum* for 24h/day and no wheel access) for ABA and FR groups, starting from PND43, increased gradually their body weight, till they reached full recovery at PND47 for FR rats and at PND49 for ABA animals.

Due to the restricted feeding schedule, daily food intake (Fig 1c) was lower in the ABA and FR rats compared with ad libitum-fed rats, CTRL and EXE. Free food availability from PND43 induced an immediate increase in food intake in both FR and ABA rats. Interestingly, ABA rats showed an increased food intake during the refeeding period at PND46 and PND47, however, they still exhibited a lower body weight than FR group (Fig 1b).

During habituation period, both EXE and ABA rats exhibited a stable voluntary wheel running measured as distance travelled on the wheel, reflecting their habituation to the apparatus. When food restriction began on PND38, the wheel activity of ABA rats constantly increased over days reaching statistical significance starting from PND40, while EXE animals maintained a stable activity (Fig 1d). Interestingly, Pearson correlation analyses showed a negative correlation between the distance travelled on the last day of ABA induction (PND42) and body weight of both ABA and EXE rats (Fig 1e).

3.1 ABA induction dysregulates the molecular composition of the glutamate synapse in the mPFC

To determine whether ABA induction altered the organization of dendritic proteins at the postsynaptic level in the mPFC, we examined the expression of the main glutamate receptors, their specific scaffolding proteins and markers of structural plasticity in the postsynaptic density (PSD) of ABA rats in the acute phase of the disorder and after a 7-days recovery period. In addition, to dissect the specific contribution of low food intake and running wheel activity on the maintenance of ABA phenotype, rodents exposed to food restriction or exercise alone were included in the analysis.

ABA rats showed reduced levels of GluN1 (Fig 2a), the obligatory subunit of NMDA receptor, in the acute phase of the pathology while the expression of GluN2A and GluN2B, the accessory subunits of NMDA receptor, were reduced only in recovered ABA rats (Fig 2b and 2c, respectively). Interestingly exercise

per sé reduced only GluN2B in the postsynaptic density of the mPFC at PND42 (Fig 2b and 2c, respectively). Regarding the analysis of AMPA receptor subunits in the PSD of mPFC, ABA rats showed reduced levels of GluA1 (Fig 2d) only in recovered ABA rats, while GluA2 levels were reduced in the acute phase of the pathology (Fig 2e). Exercise per sé increased GluA2 levels at PND42 whereas one week later, at PND49, its levels were reduced (Fig 2e).

Then, we analyzed the expression of the main scaffolding proteins of glutamate receptors, i.e. those proteins that anchor the receptors to the membrane and that are also critical for synaptic localization of newly synthesized receptor towards dendritic spines (Naisbitt *et al.* 2000) in the PSD fraction of mPFC. Akin to NMDA and AMPA receptor subunits, SAP102 [the specific scaffolding protein of NMDA receptors] (Fig 3a), SAP97 [the specific scaffolding protein of AMPA receptors] (Fig 3b) and PSD95 [an index of post-synaptic density integrity and a critical regulator of dendritic spines in vivo (Vickers *et al.* 2006)] (Fig 3c) levels were reduced only in the cortical PSD of recovered ABA rats.

Next, we evaluated the expression of filamentous F-Actin, the major cytoskeletal component of dendritic spines (Hotulainen & Hoogenraad 2010), of neuroligin-1, a postsynaptic cell-adhesion molecule at the excitatory synapse involved in synaptic transmission (Luo *et al.* 2020), and of neuronal N-cadherin, a cell-cell adhesion protein, which are all proteins involved in maintaining the structural integrity of the synapse. F-actin is differently altered depending on the phase of the pathology analyzed. In fact, weight loss reduced F-actin levels only in ABA rats (Fig 3d), while body weight recovery markedly increased them. At variance from F-actin, the neuroligin-1 levels were reduced in ABA rats despite weight recovery (Fig 3e). Moreover, neuroligin-1 levels were increased as a consequence of development. Similar to F-actin, N-cadherin levels were increased only in ABA recovered rats (Fig 3f). Food restriction and exercise per sé did not produce any change in the structural markers herein analyzed (Fig 3d, e, f), further suggesting that the composition and structure of the glutamate synapse is specifically altered by the combination of low food intake and hyperactivity.

Pearson correlation analyses were run to determine the relationship between ABA induction and the herein investigated molecular markers in the mPFC of ABA and EXE rats at both time points. As shown in figure 2, GluN1 (Fig 2g) and GluA1 (Fig 2h) negatively correlated with the distance travelled in the last day of ABA induction (PND42).

The analysis on the molecular composition of the glutamate synapse was extended to the cortical whole homogenate, in order to dissect the effect of the anorexic phenotype on glutamatergic markers translation from their availability at synaptic sites (Supplementary figures S2-S3). Interestingly, in the whole homogenate of the mPFC, exercise per sé increased the expression of GluN1, GluN2B, GluN2A and

GluA1, whereas the induction of the anorexic phenotype reduced the protein expression of GluN2B, GluN2A, GluA1, GluA2, SAP97 and F-actin only in the acute phase of the pathology. Recovery of body weight did not produce any change in the translation of the main glutamate receptors, their specific scaffolding proteins and markers of structural plasticity.

3.2 ABA induction alters structural plasticity in the mPFC

In order to evaluate the impact of the anorexic phenotype on the structural remodeling of the mPFC, we examined cortical dendritic spine density and morphology in ABA animals both at the achievement of the anorexic phenotype (acute phase) and after a period of body weight recovery using a fluorescent dyolistic labeling technique. Since the molecular analysis presented in figure 2 and 3 show that only the combination between food restriction and hyperactivity specifically alters the cortical glutamate homeostasis, we decided to focus our attention on ABA versus CTRL group in the morphological study of the mPFC. To this end, a second cohort of animals was randomly subdivided into four groups: 1) CTRL group, sacrificed at PND42; 2) ABA group, sacrificed at PND42; 3) CTRL group, sacrificed at PND49 and 4) ABA group, sacrificed at PND49.

The combination of food restriction and free wheel access reduced dendritic spine density in the acute phase, an effect that was restored after body weight recovery (Fig 4a). While no ABA-induced changes were found in dendritic spine length (Fig 4b), spine head size of ABA animals (Fig 4c), in the acute phase of the disorder, are smaller than controls; while no changes were observed in recovered ABA animals.

Further, morphological analyses of dendritic spines were performed using a highly validated method of dendritic spines classification to evaluate the shape of all protrusions (mushroom, thin, stubby and filopodia, Fig 4d). The ABA induction reduced the percentages of mushroom-shaped spines, i.e. the mature spines where the synaptic communication takes place, in the acute phase of the disorder, whereas they were increased after the recovery of body weight (Fig 4e). On the contrary, filopodia, i.e. the immature protrusions, were increased at PND42 in the mPFC of ABA rats, an effect that was restored at PND49 with body weight recovery (Fig 4h). No changes were observed in the percentages of stubby- and thin-shaped spines (Fig 4f-4g). As shown in table 2, the ABA-induced reduction of head width size in the acute phase of the pathology appeared to be widespread as it affected mushroom-, thin- and stubby-shaped spines. Again, this reduction was restored at PND49 after body weight recovery. Two-way ANOVA of spine length, classified by their shape, revealed a significant interaction ABA procedure x time only for mushroom-shaped spines (table 2): ABA induction increased the length of mushroom-shaped spines at PND42, whereas body weight recovery restored their size.

3.3 ABA induction alters the recency discrimination performance in the TOOR test

Finally, to evaluate whether temporal memory abilities in the ABA rat model may recapitulate that of anorexic patients, we exposed another cohort of CTRL and ABA rats, which reached the same behavioral phenotype presented in fig 1 (data not shown), to the temporal order object recognition test (TOOR). This cognitively-demanding test evaluates mPFC functionality through a recency recognition task, in which the animal's ability to differentiate between two familiar objects presented at different intervals is tested (Fig 5a) (Barker & Warburton 2011) (Barker *et al.* 2007; Manago *et al.* 2016).

Figure 5b represents the performance during the test phase, calculated as recency discrimination index. While CTRL rats were spending more time exploring the object presented least recently, ABA rats in the acute phase failed to show any preference for the less recent object. Interestingly, although body weight recovery ameliorated the deficit in recency discrimination in ABA rats at PND49, as compared to recency performance displayed at PND42, the temporal memory deficit still persisted.

Considering the recognition index (Fig 5c), CTRL rats explored longer the object presented in phase 1 vs. the object presented in phase 2 at both time points analyzed, as expected. On the contrary, the ABA procedure increased the exploration time of the object presented in phase 2 in respect to the one presented in phase 1 in the acute phase and after a 7-days period of recovery. In addition, impairment in recency memory is more pronounced in the acute phase of the pathology: ABA rats explored longer the object presented in phase 2 at PND42 relative to the exploration time of object presented in phase 2 in ABA-recovered rats. Moreover, animals did not show any preference in exploring the different objects in sample phase 1 or sample phase 2 nor in the test phase, as shown in the total exploration time presented in the supplementary materials (Supplementary figure S4).

To evaluate a possible association between ABA phenotype and recency memory impairment, we ran a Pearson correlation analyses between distance travelled during the last day of ABA induction and the body weight of ABA rats at both time points with the recency discrimination index. Interestingly, discrimination index correlated negatively with the distance travelled at PND42 (Fig 5d) and positively with body weight of ABA rats (Fig 5e).

4. Discussion

Adolescent ABA rats show a disorganized glutamate synapse characterized by alterations in the main glutamate receptors and their related anchoring protein together with reduced dendritic spine density in the mPFC, a combined mechanism that might contribute to explain the impairment in temporal memory recognition as shown by behavioral experiments. Moreover, although the body weight was recovered and the structural organization of dendritic spine normalized in mPFC, ABA rats still displayed reduced post-synaptic stability of AMPA and NMDA glutamate receptors associated with impaired temporal memory abilities 7 days after the end of the induction of the anorexic phenotype. These findings may help to explain, at least in part, how an imbalance in energy intake, due to the combination of caloric restriction and hyperactivity, affects the brain, thus sustaining the perpetuation of aberrant behaviors in the vicious cycle of AN.

We found that adolescent ABA rats reduced their food intake and progressively increased their physical activity leading to self-starvation and hyperactivity, further aggravating weight loss, as previously observed (Routtenberg & Kuznesof 1967; Chowdhury *et al.* 2015). The impact of free access to a running wheel on body weight became evident during the food restriction period only: rats exposed to a schedule of food restriction, exhibited limited weight loss compared to rats exposed to the combination of both conditions, despite similar food intake, pointing to hyperactivity as a key driving force to starvation (Adan *et al.* 2011). Unlike exercise animals that maintained a voluntary and stable activity during the entire experiment, when food restriction began, wheel activity of ABA rats constantly reased over days, as expected in this model (Chen *et al.* 2020; Scherma *et al.* 2017). At the end of the recovery period, the body weight of both FR and ABA rats were restored back to control levels; however, despite a higher food intake compared to FR rats, it took ABA rats more time to restore their body weight, underlying the strenuous and persistent impact of the intense physical activity in a condition of low food intake. Of note, the maladaptive cycle of self-starvation and hyperactivity in ABA rats escalated rapidly and severely in these adolescent animals, which is in agreement with the age-dependent risk for clinical AN described in the DSM-5 (DSM-V 2013).

At molecular level, the reorganization of the glutamatergic synapse in the postsynaptic density of the mPFC was specifically driven by the combination of low caloric intake and hyperactivity, since both these conditions alone did not change the expression of the glutamate markers analyzed in the active zone of the synapse. Interestingly, at PND42, physical activity per sé increased the translation of NMDA and AMPA receptor subunits, whereas hyperactivity induced by low caloric intake reduced their

expression in the whole homogenate, suggesting an increased cortical vulnerability of ABA rats. In addition, we observed that food restriction and exercise per sé did not produce any change in the structural markers analyzed (i.e. F-Actin, Neuroligin-1, N-cadherin and PSD95) in the active site of the cortical synapse, suggesting that the structure of the glutamatergic synapse is specifically altered by the combination of low food intake and hyperactivity versus the two conditions alone. At structural level, we demonstrated that the combination of weight loss and hyperactivity interfered with cortical dendritic spine formation, reducing their density and influencing their maturation in the mPFC. In fact, the reduction of mushroom-shaped spines, which represent the most active type of dendritic spines (Bourne & Harris 2007), and the increase of filopodia, i.e. the immature dendritic protrusions, may be indicative of an increased turnover of the immature dendritic structures reducing the communicative synapses and their strengthening and suggesting a mechanism to explain the cognitive deficits observed in anorexic patients (Olivo et al. 2019). In addition, the reduced spine density in the mPFC of ABA rats was coupled with a reduced head diameter, reflecting a shrinkage of the postsynaptic density (Hering & Sheng 2001) and an impaired glutamatergic signaling via reduced expression and synaptic retention of specific glutamate receptors. Interestingly, such alterations are paralleled by reduced expression and altered synaptic localization of structural markers such as F-actin. Since synaptic function is positively associated with spine head volume, the PSD area and the number of glutamate receptors (Bosch & Hayashi 2012), our data revealed that the molecular dysregulation of the glutamate synapse observed at the achievement of the anorexic phenotype correlates with ABA-induced hyperactive behavior and not with body weight (data not shown), further corroborating the AN-induced weakening of synaptic strength in the mPFC.

Of note, seven days of refeeding restored body weight and the observed structural alterations in the mPFC, even increasing the percentages of mushroom-shaped spine. Such effect may reflect an adaptive response, or at least an attempt, of the mature synapses to restore a physiological synaptic communication. This is in line with the observation that, in humans, adolescent anorexic subjects display reduced grey matter volumes in the prefrontal cortex, decreased cortical thickness and subcortical volumes compared to healthy controls, an effect only partially retrieved upon refeeding (Kaufmann et al. 2020; Frintrop et al. 2019; Martin Monzon et al. 2017). Despite weight recovery canceled structural changes induced by the ABA phenotype, cytoskeletal instability in the mPFC of ABA rats is further confirmed at the molecular level via reduction of neuroligin-1 and PSD95, suggesting that these molecular alterations may account for functional persistent changes, as previously suggested in the mPFC of ABA rats even for the endocannabinoid system (Collu et al. 2019). Moreover, an overall reduction of

the glutamatergic signaling in the postsynaptic density of the mPFC was still observed, indicating a profound and persistent reorganization of the postsynaptic density composition. These data demonstrate an impaired synaptic localization of the main glutamate NMDA and AMPA receptor subunits since their expression was significantly reduced in the PSD fraction, but not in the whole cortical homogenate: accordingly, it appears that ABA induction has not influenced the translation process of these receptors but, rather, their synaptic retention. Since SAP102 and SAP97 in the postsynaptic density are essential for the synaptic localization of AMPA and NMDA receptors (Kim *et al.* 2005; Vickers *et al.* 2006) and for anchoring such receptors to the postsynaptic membrane, the herein observed reduction indicates impaired delivery and reduced synaptic stability of glutamate receptors at the postsynaptic membrane.

Taken together, the complex set of structural and molecular analyses herein shown point to (mal)adaptive glutamatergic rearrangements occurring in the adolescent brain, which might contribute to alter the incentive motivational system and recency discrimination abilities to drive maladaptive behaviors in AN, as revealed by the significant correlations between glutamatergic receptors and recency discrimination index with ABA-induced hyperactive behavior and body weight loss. These events are functionally relevant since the long-term failure in recruiting critical glutamate determinants at synaptic level might reduce the transition to active dendritic spines, leading to a functional destabilization of the mPFC and conferring greater vulnerability to AN patients. This notion is reinforced by the evidence that the recency discrimination index in the temporal order object recognition test, which requires an intact and functional mPFC (Barker *et al.* 2007), was impaired. The dysregulated compartmentalization and reduced synaptic retention of critical glutamate determinants, as a result of the anorexic phenotype, indicate that, at the beginning of the TOOR test, the availability of NMDA and AMPA receptors at active synaptic sites is reduced in the mPFC of ABA rats, a deficiency that may contribute to the memory impairment observed in both ABA rats and AN patients (Amianto *et al.* 2013; Biezonski *et al.* 2016; Lamanna *et al.* 2019). In addition, weight recovery in ABA rats is not paralleled by memory recovery: in fact, a recency memory deficit is still present following the recovery period, suggesting a vulnerability trait for relapse. This possibility is corroborated by the evidence of a slower maturation of the prefrontal regulatory circuitry in AN patients, as shown by fMRI studies (Xu *et al.* 2017), in which AN adolescents exhibited altered maturation of the executive network, leading to impaired cognitive flexibility and working memory (Olivo *et al.* 2019; Bohon *et al.* 2020; Fuglset 2019). Moreover, since the object recognition task is dependent on a network of brain areas that interact and potentially contribute to recognition memory (Warburton & Brown 2015), we cannot rule out that changes in other brain regions of the circuitry in which mPFC is embedded (such as perirhinal cortex, hippocampus and medial dorsal

thalamus) might contribute to the observed behavioral changes. Interestingly, in this scenario Milton and colleagues elegantly showed that body weight loss and reversal learning in ABA rats was prevented via chemogenetic suppression of the mPFC-nucleus accumbens shell pathway (Milton *et al.* 2020), suggesting that different cognitive domains might be involved in AN.

Although we are aware that the TOOR test cannot represent cognition in its entirety, however these data represent one of the first lines of evidence of cognitive impairments in experimental models of AN, in line with results observed in AN patients. Thus, in order to better characterize ABA-related cognitive alterations, future behavioral studies will investigate other cognitive domain in experimental models

5. Conclusions

Even though we are aware that no animal model can fully mimic a complex psychiatric disorder such as AN and that possible developmental effects might occur during adolescence, the ABA model has the potential to provide useful insights into the mechanisms underlying the development and maintenance of these maladaptive behaviors, despite the overall alteration in glutamate homeostasis herein shown is rather mild (Lamanna *et al.* 2019; Gutierrez 2013). Our data indicate that the combination between food restriction and hyperactivity leads to memory dysfunction, associated with an altered composition and structure of the glutamatergic synapse in the mPFC.

The PFC is known as a site of integration of numerous stimuli with a key role in converting them into efferent signals that contribute toward executive functioning, cognitive flexibility, memory and reward-related response (Dalley *et al.* 2004; Dalton *et al.* 2016): along this line of reasoning it appears that interfering with its homeostasis may contribute, at least in part, to drive and sustain AN-induced behaviors. In line with recent data that demonstrate that mPFC activity controls hyperactivity under food restriction conditions (Santiago *et al.* 2021), we showed that the combination of low BMI and hyperactivity status are key factors in driving recency memory impairment whereas weight restoration does not seem to effectively rescue such alterations. Consequently, the deviation from normal brain development, and particularly the impairment in the structure and composition of the excitatory synapse in the mPFC, reflective of a pathological-like state and not of a generalized effect of malnutrition or exercise, might contribute to sustain the maintenance of aberrant behaviors, and establish a vicious cycle, perpetuating restraint over-eating and other AN-related behaviors. In this scenario, our data might pave the way toward new pharmacotherapies designed to manipulate the glutamate system and restore normal cognitive functions. Finally, given the neurobiological differences that we observed between the

acute phase of the AN phenotype and after recovery, future studies will try to get further insights into the mechanisms that govern the difference between these two phases of the disorder.

```
--Human subjects --
Involves human subjects:
If yes: Informed consent & ethics approval achieved:
```
=> if yes, please ensure that the info "Informed consent was achieved for all subjects, and the experiments were approved by the local ethics committee." is included in the Methods.

```
ARRIVE guidelines have been followed:
Yes
=> if it is a Review or Editorial, skip complete sentence => if No, include a
statement in the "Conflict of interest disclosure" section: "ARRIVE guidelines
were not followed for the following reason:
"
(edit phrasing to form a complete sentence as necessary).
=> if Yes, insert in the "Conflict of interest disclosure" section:
"All experiments were conducted in compliance with the ARRIVE guidelines."
unless it is a Review or Editorial

Conflicts of interest:  none
=> if 'none', insert "The authors have no conflict of interest to declare."
=> else insert info unless it is already included

Open Science Badges
No, I am not interested to achieve Open Science Badge(s) => if yes, please see
Comments from the Journal for further information => if no, no information needs
to be included in the manuscript.
```

Author contributions

FM, FF and LC conceptualized the research; FM, FF and LC performed data curation and formal analysis; FM and GT performed western blot analysis; FM, GT, GB and BT performed morphological analysis; FM, GT and LC analyzed and curated data; FM, GB, GT, BT, FF and LC wrote, reviewed and edited the paper. LC acquired funding for the project.

Conflict of Interest

The authors declare no conflict of interest.

References

Adan, R. A., Hillebrand, J. J., Danner, U. N., Cardona Cano, S., Kas, M. J. and Verhagen, L. A. (2011) Neurobiology driving hyperactivity in activity-based anorexia. *Curr Top Behav Neurosci* **6,** 229-250. 10.1007/7854_2010_77.

Amianto, F., Caroppo, P., D'Agata, F. et al. (2013) Brain volumetric abnormalities in patients with anorexia and bulimia nervosa: a voxel-based morphometry study. *Psychiatry Res* **213,** 210-216. 10.1016/j.pscychresns.2013.03.010.

Aoki, C., Chowdhury, T. G., Wable, G. S. and Chen, Y. W. (2017) Synaptic changes in the hippocampus of adolescent female rodents associated with resilience to anxiety and suppression of food restriction-evoked hyperactivity in an animal model for anorexia nervosa. *Brain Res* **1654,** 102-115. 10.1016/j.brainres.2016.01.019.

Arcelus, J., Mitchell, A. J., Wales, J. and Nielsen, S. (2011) Mortality rates in patients with anorexia nervosa and other eating disorders. A meta-analysis of 36 studies. *Arch Gen Psychiatry* **68,** 724-731. 10.1001/archgenpsychiatry.2011.74.

Barbarich-Marsteller, N. C., Underwood, M. D., Foltin, R. W., Myers, M. M., Walsh, B. T., Barrett, J. S. and Marsteller, D. A. (2013) Identifying novel phenotypes of vulnerability and resistance to activity-based anorexia in adolescent female rats. *Int J Eat Disord* **46,** 737-746. 10.1002/eat.22149.

Barker, G. R., Bird, F., Alexander, V. and Warburton, E. C. (2007) Recognition memory for objects, place, and temporal order: a disconnection analysis of the role of the medial prefrontal cortex and perirhinal cortex. *J Neurosci* **27,** 2948-2957. 10.1523/JNEUROSCI.5289-06.2007.

Barker, G. R. and Warburton, E. C. (2011) Evaluating the neural basis of temporal order memory for visual stimuli in the rat. *Eur J Neurosci* **33,** 705-716. 10.1111/j.1460-9568.2010.07555.x.

Berends, T., van Meijel, B., Nugteren, W., Deen, M., Danner, U. N., Hoek, H. W. and van Elburg, A. A. (2016) Rate, timing and predictors of relapse in patients with anorexia nervosa following a relapse prevention program: a cohort study. *BMC Psychiatry* **16,** 316. 10.1186/s12888-016-1019-y.

Biezonski, D., Cha, J., Steinglass, J. and Posner, J. (2016) Evidence for Thalamocortical Circuit Abnormalities and Associated Cognitive Dysfunctions in Underweight Individuals with Anorexia Nervosa. *Neuropsychopharmacology* **41,** 1560-1568. 10.1038/npp.2015.314.

Bohon, C., Weinbach, N. and Lock, J. (2020) Performance and brain activity during the Wisconsin Card Sorting Test in adolescents with obsessive-compulsive disorder and adolescents with weight-restored anorexia nervosa. *Eur Child Adolesc Psychiatry* **29,** 217-226. 10.1007/s00787-019-01350-4.

Bosch, M. and Hayashi, Y. (2012) Structural plasticity of dendritic spines. *Curr Opin Neurobiol* **22,** 383-388. 10.1016/j.conb.2011.09.002.

Bourne, J. and Harris, K. M. (2007) Do thin spines learn to be mushroom spines that remember? *Curr Opin Neurobiol* **17,** 381-386. 10.1016/j.conb.2007.04.009.

Caffino, L., Giannotti, G., Malpighi, C., Racagni, G. and Fumagalli, F. (2015) Short-term withdrawal from developmental exposure to cocaine activates the glucocorticoid receptor and alters spine dynamics. *Eur Neuropsychopharmacol* **25,** 1832-1841. 10.1016/j.euroneuro.2015.05.002.

Caffino, L., Mottarlini, F., Mingardi, J., Zita, G., Barbon, A. and Fumagalli, F. (2020a) Anhedonic-like behavior and BDNF dysregulation following a single injection of cocaine during adolescence. *Neuropharmacology* **175,** 108161. 10.1016/j.neuropharm.2020.108161.

Caffino, L., Piva, A., Giannotti, G., Di Chio, M., Mottarlini, F., Venniro, M., Yew, D. T., Chiamulera, C. and Fumagalli, F. (2017) Ketamine Self-Administration Reduces the Homeostasis of the Glutamate Synapse in the Rat Brain. *Mol Neurobiol* **54,** 7186-7193. 10.1007/s12035-016-0231-6.

Caffino, L., Verheij, M. M. M., Roversi, K. et al. (2020b) Hypersensitivity to amphetamine's psychomotor and reinforcing effects in serotonin transporter knockout rats: Glutamate in the nucleus accumbens. *Br J Pharmacol*. 10.1111/bph.15211.

Carrera, O., Fraga, A., Pellon, R. and Gutierrez, E. (2014) Rodent model of activity-based anorexia. *Curr Protoc Neurosci* **67,** 9 47 41-11. 10.1002/0471142301.ns0947s67.

Chapman, R. H. and Stern, J. M. (1978) Maternal stress and pituitary-adrenal manipulations during pregnancy in rats: effects on morphology and sexual behavior of male offspring. *J Comp Physiol Psychol* **92,** 1074-1083. 10.1037/h0077509.

Chen, Y. W., Actor-Engel, H., Sherpa, A. D., Klingensmith, L., Chowdhury, T. G. and Aoki, C. (2020) Correction to: NR2A- and NR2B-NMDA receptors and drebrin within postsynaptic spines of the hippocampus correlate with hunger-evoked exercise. *Brain Struct Funct* **225,** 1165. 10.1007/s00429-020-02030-9.

Chen, Y. W., Wable, G. S., Chowdhury, T. G. and Aoki, C. (2016) Enlargement of Axo-Somatic Contacts Formed by GAD-Immunoreactive Axon Terminals onto Layer V Pyramidal Neurons in the Medial Prefrontal Cortex of Adolescent Female Mice Is Associated with Suppression of Food Restriction-Evoked Hyperactivity and Resilience to Activity-Based Anorexia. *Cereb Cortex* **26,** 2574-2589. 10.1093/cercor/bhv087.

Chowdhury, T. G., Barbarich-Marsteller, N. C., Chan, T. E. and Aoki, C. (2014) Activity-based anorexia has differential effects on apical dendritic branching in dorsal and ventral hippocampal CA1. *Brain Struct Funct* **219,** 1935-1945. 10.1007/s00429-013-0612-9.

Chowdhury, T. G., Chen, Y. W. and Aoki, C. (2015) Using the Activity-based Anorexia Rodent Model to Study the Neurobiological Basis of Anorexia Nervosa. *J Vis Exp*, e52927. 10.3791/52927.

Collu, R., Scherma, M., Piscitelli, F. et al. (2019) Impaired brain endocannabinoid tone in the activity-based model of anorexia nervosa. *Int J Eat Disord* **52,** 1251-1262. 10.1002/eat.23157.

Cowdrey, F. A., Filippini, N., Park, R. J., Smith, S. M. and McCabe, C. (2014) Increased resting state functional connectivity in the default mode network in recovered anorexia nervosa. *Hum Brain Mapp* **35,** 483-491. 10.1002/hbm.22202.

Dalley, J. W., Theobald, D. E., Bouger, P., Chudasama, Y., Cardinal, R. N. and Robbins, T. W. (2004) Cortical cholinergic function and deficits in visual attentional performance in rats following 192 IgG-saporin-induced lesions of the medial prefrontal cortex. *Cereb Cortex* **14,** 922-932. 10.1093/cercor/bhh052.

Dalton, G. L., Wang, N. Y., Phillips, A. G. and Floresco, S. B. (2016) Multifaceted Contributions by Different Regions of the Orbitofrontal and Medial Prefrontal Cortex to Probabilistic Reversal Learning. *J Neurosci* **36,** 1996-2006. 10.1523/JNEUROSCI.3366-15.2016.

DSM-V (2013) *Diagnostic and Statistical Manual of Mental Disorders: DSM-V. Washington DC: American Psychiatric Association*.

Ehrlich, S., Geisler, D., Ritschel, F. et al. (2015) Elevated cognitive control over reward processing in recovered female patients with anorexia nervosa. *J Psychiatry Neurosci* **40,** 307-315. 10.1503/jpn.140249.

Foldi, C. J., Milton, L. K. and Oldfield, B. J. (2017) The Role of Mesolimbic Reward Neurocircuitry in Prevention and Rescue of the Activity-Based Anorexia (ABA) Phenotype in Rats. *Neuropsychopharmacology* **42,** 2292-2300. 10.1038/npp.2017.63.

Frank, G. K. W., DeGuzman, M. C., Shott, M. E., Laudenslager, M. L., Rossi, B. and Pryor, T. (2018) Association of Brain Reward Learning Response With Harm Avoidance, Weight Gain, and Hypothalamic Effective Connectivity in Adolescent Anorexia Nervosa. *JAMA Psychiatry* **75,** 1071-1080. 10.1001/jamapsychiatry.2018.2151.

Friederich, H. C., Wu, M., Simon, J. J. and Herzog, W. (2013) Neurocircuit function in eating disorders. *Int J Eat Disord* **46,** 425-432. 10.1002/eat.22099.

Frintrop, L., Trinh, S., Liesbrock, J. et al. (2019) The reduction of astrocytes and brain volume loss in anorexia nervosa-the impact of starvation and refeeding in a rodent model. *Transl Psychiatry* **9,** 159. 10.1038/s41398-019-0493-7.

Fuglset, T. S. (2019) Set-shifting, central coherence and decision-making in individuals recovered from anorexia nervosa: a systematic review. *J Eat Disord* **7,** 22. 10.1186/s40337-019-0251-5.

Gardoni, F., Saraceno, C., Malinverno, M., Marcello, E., Verpelli, C., Sala, C. and Di Luca, M. (2012) The neuropeptide PACAP38 induces dendritic spine remodeling through ADAM10-N-cadherin signaling pathway. *J Cell Sci* **125,** 1401-1406. 10.1242/jcs.097576.

Godlewska, B. R., Pike, A., Sharpley, A. L., Ayton, A., Park, R. J., Cowen, P. J. and Emir, U. E. (2017) Brain glutamate in anorexia nervosa: a magnetic resonance spectroscopy case control study at 7 Tesla. *Psychopharmacology (Berl)* **234,** 421-426. 10.1007/s00213-016-4477-5.

Gutierrez, E. (2013) A rat in the labyrinth of anorexia nervosa: contributions of the activity-based anorexia rodent model to the understanding of anorexia nervosa. *Int J Eat Disord* **46,** 289-301. 10.1002/eat.22095.

Harris, K. M., Jensen, F. E. and Tsao, B. (1992) Three-dimensional structure of dendritic spines and synapses in rat hippocampus (CA1) at postnatal day 15 and adult ages: implications for the maturation of synaptic physiology and long-term potentiation. *J Neurosci* **12,** 2685-2705.

Hering, H. and Sheng, M. (2001) Dendritic spines: structure, dynamics and regulation. *Nat Rev Neurosci* **2,** 880-888. 10.1038/35104061.

Hildebrandt, T., Grotzinger, A., Reddan, M., Greif, R., Levy, I., Goodman, W. and Schiller, D. (2015) Testing the disgust conditioning theory of food-avoidance in adolescents with recent onset anorexia nervosa. *Behav Res Ther* **71,** 131-138. 10.1016/j.brat.2015.06.008.

Himmerich, H., Kan, C., Au, K. and Treasure, J. (2020) Pharmacological treatment of eating disorders, comorbid mental health problems, malnutrition and physical health consequences. *Pharmacol Ther***,** 107667. 10.1016/j.pharmthera.2020.107667.

Ho, E. V., Klenotich, S. J., McMurray, M. S. and Dulawa, S. C. (2016) Activity-Based Anorexia Alters the Expression of BDNF Transcripts in the Mesocorticolimbic Reward Circuit. *PLoS One* **11,** e0166756. 10.1371/journal.pone.0166756.

Hotulainen, P. and Hoogenraad, C. C. (2010) Actin in dendritic spines: connecting dynamics to function. *J Cell Biol* **189,** 619-629. 10.1083/jcb.201003008.

Kaufmann, L. K., Hanggi, J., Jancke, L., Baur, V., Piccirelli, M., Kollias, S., Schnyder, U., Martin-Soelch, C. and Milos, G. (2020) Age influences structural brain restoration during weight gain therapy in anorexia nervosa. *Transl Psychiatry* **10,** 126. 10.1038/s41398-020-0809-7.

Kaye, W. (2008) Neurobiology of anorexia and bulimia nervosa. *Physiol Behav* **94,** 121-135. 10.1016/j.physbeh.2007.11.037.

Kim, M. J., Dunah, A. W., Wang, Y. T. and Sheng, M. (2005) Differential roles of NR2A- and NR2B-containing NMDA receptors in Ras-ERK signaling and AMPA receptor trafficking. *Neuron* **46,** 745-760. 10.1016/j.neuron.2005.04.031.

Klump, K. L. (2013) Puberty as a critical risk period for eating disorders: a review of human and animal studies. *Horm Behav* **64,** 399-410. 10.1016/j.yhbeh.2013.02.019.

Kullmann, S., Giel, K. E., Teufel, M., Thiel, A., Zipfel, S. and Preissl, H. (2014) Aberrant network integrity of the inferior frontal cortex in women with anorexia nervosa. *Neuroimage Clin* **4,** 615-622. 10.1016/j.nicl.2014.04.002.

Lamanna, J., Sulpizio, S., Ferro, M., Martoni, R., Abutalebi, J. and Malgaroli, A. (2019) Behavioral assessment of activity-based-anorexia: how cognition can become the drive wheel. *Physiol Behav* **202,** 1-7. 10.1016/j.physbeh.2019.01.016.

Lipsman, N., Woodside, D. B. and Lozano, A. M. (2015) Neurocircuitry of limbic dysfunction in anorexia nervosa. *Cortex* **62,** 109-118. 10.1016/j.cortex.2014.02.020.

Lock, J., Garrett, A., Beenhakker, J. and Reiss, A. L. (2011) Aberrant brain activation during a response inhibition task in adolescent eating disorder subtypes. *Am J Psychiatry* **168,** 55-64. 10.1176/appi.ajp.2010.10010056.

Luo, J., Tan, J. M. and Nithianantharajah, J. (2020) A molecular insight into the dissociable regulation of associative learning and motivation by the synaptic protein neuroligin-1. *BMC Biol* **18,** 118. 10.1186/s12915-020-00848-7.

Manago, F., Mereu, M., Mastwal, S. et al. (2016) Genetic Disruption of Arc/Arg3.1 in Mice Causes Alterations in Dopamine and Neurobehavioral Phenotypes Related to Schizophrenia. *Cell Rep* **16,** 2116-2128. 10.1016/j.celrep.2016.07.044.

Martin Monzon, B., Henderson, L. A., Madden, S., Macefield, V. G., Touyz, S., Kohn, M. R., Clarke, S., Foroughi, N. and Hay, P. (2017) Grey matter volume in adolescents with anorexia nervosa and associated eating disorder symptoms. *Eur J Neurosci* **46,** 2297-2307. 10.1111/ejn.13659.

Micali, N. and Dahlgren, C. L. (2016) All that glisters is not an endophenotype: rethinking endophenotypes in anorexia nervosa. *Eur Child Adolesc Psychiatry* **25,** 1149-1150. 10.1007/s00787-016-0910-x.

Milton, L. K., Mirabella, P. N., Greaves, E., Spanswick, D. C., van den Buuse, M., Oldfield, B. J. and Foldi, C. J. (2020) Suppression of Corticostriatal Circuit Activity Improves Cognitive Flexibility and Prevents Body Weight Loss in Activity-Based Anorexia in Rats. *Biol Psychiatry*. 10.1016/j.biopsych.2020.06.022.

Monteleone, A. M., Castellini, G., Volpe, U., Ricca, V., Lelli, L., Monteleone, P. and Maj, M. (2018) Neuroendocrinology and brain imaging of reward in eating disorders: A possible key to the treatment of anorexia nervosa and bulimia nervosa. *Prog Neuropsychopharmacol Biol Psychiatry* **80,** 132-142. 10.1016/j.pnpbp.2017.02.020.

Mottarlini, F., Bottan, G., Tarenzi, B., Colciago, A., Fumagalli, F. and Caffino, L. (2020) Activity-Based Anorexia Dynamically Dysregulates the Glutamatergic Synapse in the Nucleus Accumbens of Female Adolescent Rats. *Nutrients* **12**. 10.3390/nu12123661.

Murray, S. L. and Holton, K. F. (2021) Post-traumatic stress disorder may set the neurobiological stage for eating disorders: A focus on glutamatergic dysfunction. *Appetite* **167,** 105599. 10.1016/j.appet.2021.105599.

Nagl, M., Jacobi, C., Paul, M., Beesdo-Baum, K., Hofler, M., Lieb, R. and Wittchen, H. U. (2016) Prevalence, incidence, and natural course of anorexia and bulimia nervosa among adolescents and young adults. *Eur Child Adolesc Psychiatry* **25,** 903-918. 10.1007/s00787-015-0808-z.

Naisbitt, S., Valtschanoff, J., Allison, D. W., Sala, C., Kim, E., Craig, A. M., Weinberg, R. J. and Sheng, M. (2000) Interaction of the postsynaptic density-95/guanylate kinase domain-associated protein complex with a light chain of myosin-V and dynein. *J Neurosci* **20,** 4524-4534.

Nikendei, C., Funiok, C., Pfuller, U., Zastrow, A., Aschenbrenner, S., Weisbrod, M., Herzog, W. and Friederich, H. C. (2011) Memory performance in acute and weight-restored anorexia nervosa patients. *Psychol Med* **41,** 829-838. 10.1017/S0033291710001121.

Ohrmann, P., Kersting, A., Suslow, T., Lalee-Mentzel, J., Donges, U. S., Fiebich, M., Arolt, V., Heindel, W. and Pfleiderer, B. (2004) Proton magnetic resonance spectroscopy in anorexia nervosa: correlations with cognition. *Neuroreport* **15,** 549-553. 10.1097/00001756-200403010-00033.

Olivo, G., Gaudio, S. and Schioth, H. B. (2019) Brain and Cognitive Development in Adolescents with Anorexia Nervosa: A Systematic Review of fMRI Studies. *Nutrients* **11**. 10.3390/nu11081907.

Paxinos, G. and Watson, C. (2013) *The Rat Brain in Stereotaxic Coordinates 7th Edition*. Eselvier.

Reville, M. C., O'Connor, L. and Frampton, I. (2016) Literature Review of Cognitive Neuroscience and Anorexia Nervosa. *Curr Psychiatry Rep* **18,** 18. 10.1007/s11920-015-0651-4.

Routtenberg, A. and Kuznesof, A. W. (1967) Self-starvation of rats living in activity wheels on a restricted feeding schedule. *J Comp Physiol Psychol* **64,** 414-421. 10.1037/h0025205.

Sakurai, T. and Gamo, N. J. (2019) Cognitive functions associated with developing prefrontal cortex during adolescence and developmental neuropsychiatric disorders. *Neurobiol Dis* **131,** 104322. 10.1016/j.nbd.2018.11.007.

Sanders, N., Smeets, P. A., van Elburg, A. A., Danner, U. N., van Meer, F., Hoek, H. W. and Adan, R. A. (2015) Altered food-cue processing in chronically ill and recovered women with anorexia nervosa. *Front Behav Neurosci* **9,** 46. 10.3389/fnbeh.2015.00046.

Santiago, A. N., Makowicz, E. A., Du, M. and Aoki, C. (2021) Food Restriction Engages Prefrontal Corticostriatal Cells and Local Microcircuitry to Drive the Decision to Run versus Conserve Energy. *Cereb Cortex* **31,** 2868-2885. 10.1093/cercor/bhaa394.

Sato, Y., Saito, N., Utsumi, A., Aizawa, E., Shoji, T., Izumiyama, M., Mushiake, H., Hongo, M. and Fukudo, S. (2013) Neural basis of impaired cognitive flexibility in patients with anorexia nervosa. *PLoS One* **8,** e61108. 10.1371/journal.pone.0061108.

Schalla, M. A. and Stengel, A. (2019) Activity Based Anorexia as an Animal Model for Anorexia Nervosa-A Systematic Review. *Front Nutr* **6,** 69. 10.3389/fnut.2019.00069.

Scherma, M., Collu, R., Satta, V., Giunti, E. and Fadda, P. (2019) Animal Models of Eating Disorders. *Methods Mol Biol* **2011,** 297-314. 10.1007/978-1-4939-9554-7_17.

Scherma, M., Satta, V., Collu, R., Boi, M. F., Usai, P., Fratta, W. and Fadda, P. (2017) Cannabinoid CB1 /CB2 receptor agonists attenuate hyperactivity and body weight loss in a rat model of activity-based anorexia. *Br J Pharmacol* **174,** 2682-2695. 10.1111/bph.13892.

Schmidt, N. M., Glymour, M. M. and Osypuk, T. L. (2017) Adolescence Is a Sensitive Period for Housing Mobility to Influence Risky Behaviors: An Experimental Design. *J Adolesc Health* **60,** 431-437. 10.1016/j.jadohealth.2016.10.022.

Sullivan, P. F. (1995) Mortality in anorexia nervosa. *Am J Psychiatry* **152,** 1073-1074. 10.1176/ajp.152.7.1073.

van Kuyck, K., Casteels, C., Vermaelen, P., Bormans, G., Nuttin, B. and Van Laere, K. (2007) Motor- and food-related metabolic cerebral changes in the activity-based rat model for anorexia nervosa: a voxel-based microPET study. *Neuroimage* **35,** 214-221. 10.1016/j.neuroimage.2006.12.009.

Vickers, C. A., Stephens, B., Bowen, J., Arbuthnott, G. W., Grant, S. G. and Ingham, C. A. (2006) Neurone specific regulation of dendritic spines in vivo by post synaptic density 95 protein (PSD-95). *Brain Res* **1090,** 89-98. 10.1016/j.brainres.2006.03.075.

Warburton, E. C. and Brown, M. W. (2015) Neural circuitry for rat recognition memory. *Behav Brain Res* **285,** 131-139. 10.1016/j.bbr.2014.09.050.

Wierenga, C. E., Ely, A., Bischoff-Grethe, A., Bailer, U. F., Simmons, A. N. and Kaye, W. H. (2014) Are Extremes of Consumption in Eating Disorders Related to an Altered Balance between Reward and Inhibition? *Front Behav Neurosci* **8,** 410. 10.3389/fnbeh.2014.00410.

Xu, J., Harper, J. A., Van Enkevort, E. A., Latimer, K., Kelley, U. and McAdams, C. J. (2017) Neural activations are related to body-shape, anxiety, and outcomes in adolescent anorexia nervosa. *J Psychiatr Res* **87,** 1-7. 10.1016/j.jpsychires.2016.12.005.

Yau, W. Y., Bischoff-Grethe, A., Theilmann, R. J., Torres, L., Wagner, A., Kaye, W. H. and Fennema-Notestine, C. (2013) Alterations in white matter microstructure in women recovered from anorexia nervosa. *Int J Eat Disord* **46,** 701-708. 10.1002/eat.22154.

Zink, C. F. and Weinberger, D. R. (2010) Cracking the moody brain: the rewards of self starvation. *Nat Med* **16,** 1382-1383. 10.1038/nm1210-1382.

Figure legends

Figure 1. Schematic representation of the experimental paradigm performed in female adolescent rats to induce the activity-based anorexia (ABA) phenotype (a), average daily body weight (b), food intake (c) and total daily distance travelled (d) in CTRL, FR, EXE and ABA rats. Panel (e) shows the Pearson's product–moment correlation (*r*) analyses between body weight and distance travelled at post-natal day (PND)42 of ABA and EXE rats.

Results are presented as the mean ± SEM.

p<0.0001 FR and ABA vs CTRL and EXE; *p<0.05 ABA vs FR; °p<0.05, °°p<0.01, °°°p<0.001 ABA vs CTRL; £p<0.05, ££p<0.01, £££p<0.001 FR vs CTRL; $p<0.05, $$p<0.01, $$$p<0.001 ABA vs EXE, §§p<0.01 CTRL vs EXE (two-way ANOVA with repeated measures followed by Bonferroni's multiple comparisons test)

CTRL=control; FR=food-restricted; EXE=exercise; ABA=activity-based anorexia

Figure 2. Effect of the ABA protocol on the NMDA and AMPA receptor subunits expression in the post-synaptic density (PSD) of the medial prefrontal cortex (mPFC) in the acute phase of the pathology (PND42) and after a 7-days recovery period (PND49).

Protein levels of the obligatory subunit GluN1 (a) and the accessory subunits GluN2A (b) and GluN2B (c) of NMDA receptors, and of GluA1 (d) and GluA2 (e) subunits of AMPA receptors are expressed as percentages of controls sacrificed at PND42 and represent the mean ± SEM of five-six rats per group. Panel (f) shows representative immunoblots for GluN1, GluN2A, GluN2B, GluA1 and GluA2 proteins in the PSD of mPFC. Pearson's product–moment correlation (*r*) analyses between distance travelled at PND42 and GluN1 (g) and GluA1 (h) protein levels of ABA and EXE rats.

**p<0.01 vs. CTRL-acute phase, $p<0.05, $$p<0.01, $$$p<0.001 vs. CTRL-recovery, §§p<0.01 vs. FR-acute phase, @@p<0.01, @@@p<0.001 vs. EXE-acute phase, £p<0.05, ££p<0.01, £££p<0.001 vs ABA-acute phase, °p<0.05, °°p<0.01, °°°p<0.001 vs FR-recovery, ++p<0.01, +++p<0.001 vs EXE-recovery, ###p<0.001 vs ABA-recovery (three-way ANOVA or two-way ANOVA followed by Bonferroni's multiple comparisons test).

CTRL=control; FR=food-restricted; EXE=exercise; ABA=activity-based anorexia

Figure 3. Effect of the ABA protocol on scaffolding proteins and on synaptic structural markers expression in the PSD of mPFC in the acute phase of the pathology (PND42) and after a 7-days recovery period (PND49).

Protein levels of SAP102 (a), SAP97 (b), PSD95 (c), filamentous (F-)Actin (d), neuroligin-1 (e) and N-cadherin (f) are expressed as percentages of controls sacrificed at PND42 and represent the mean ± SEM of five-six rats per group. Panel (g) shows representative immunoblots for SAP102, SAP97, PSD95, F-actin, neuroligin-1 and N-cadherin proteins in the PSD of mPFC.

*p<0.05, ***p<0.001 vs. CTRL-acute phase, $p<0.05, $$p<0.01, $$$p<0.001 vs. CTRL-recovery, £p<0.05, £££p<0.001 vs ABA-acute phase, °p<0.05, °°p<0.01, °°°p<0.001 vs FR-recovery, +p<0.05, ++p<0.01, +++p<0.001 vs EXE-recovery (three-way ANOVA or two-way ANOVA followed by Bonferroni's multiple

comparisons test).

CTRL=control; FR=food-restricted; EXE=exercise; ABA=activity-based anorexia

Figure 4. Effects of ABA induction on dendritic spine density and morphology in the mPFC measured in the acute phase of the pathology (PND42) and after a 7-days recovery period (PND49).

Panel a shows total spine density in the mPFC and, below the graph, representative images of dendrite segments from the mPFC of CTRL and ABA animals evaluated at PND42 (left) and PND49 (right). Average spines length and average spines head width of the total spines measured are shown in panel b and c, respectively. The percentage of total protrusions belonging to different categories depending on their morphology (d) is presented for mushroom- (e), stubby- (f), thin- (g) and filopodia (h)-shaped protrusions.

n > 3000 spines from at least 28 different neurons for each group, around 5 dendritic segments for each hemisphere, 8 hemispheres/group

Results are presented as the mean ± SEM.

*p<0.05. vs. CTRL-acute phase; $^\#$p<0.05, $^{\#\#}$p<0.01, $^{\#\#\#}$p<0.001 vs ABA-recovery, ‡p<0.05 vs CTRL-recovery (two-way ANOVA followed by Bonferroni's multiple comparisons test).

CTRL=control; ABA=activity-based anorexia

Figure 5. Schematic representation of the temporal order object recognition (TOOR) test performed in female adolescent CTRL and ABA rats (a) in the acute phase of the pathology (PND42) and after a 7-days period of recovery (PND49). Recency discrimination index (b) and recognition index (c) measured during the test phase of the TOOR test. Pearson's product–moment correlation (*r*) analyses between recency discrimination index and distance travelled at PND42 of ABA rats (d). Pearson's product–moment correlation (*r*) analyses between recency discrimination index and body weight (e) of ABA and CTRL rats at both PND42 and PND49.

Recency discrimination index was calculated as (exploration time of object presented in sample phase 1 ─ exploration time of object presented in sample phase 2) / total time spent exploring both objects in the test phase.

***p<0.001 vs CTRL-acute phase; ‡p<0.05, vs. CTRL-recovery; $^\#$p<0.05 vs ABA- acute phase (two-way ANOVA followed by Fisher's LSD test).

Recognition index was calculated as exploration time during the test phase of Object 1 or Object 2/(Object 1 + Object 2 exploration time)*100 at PND42 (left) or at PND49 (right).

$^{@@@}$p<0.001 vs Object 1-CTRL acute phase; §p<0.05 vs Object 1-CTRL recovery; ***p<0.001 vs Object 1-ABA acute phase; $^{\#\#\#}$p<0.001 vs Object 2-CTRL acute phase; ‡p<0.05 vs Object 2-ABA recovery; $^\circ$p<0.05 vs Object 1-ABA recovery; $^\pounds$p<0.05 vs Object 2-CTRL recovery (two-way ANOVA followed by Fisher's LSD test).

Histograms represent the mean ± SEM of at least seven rats per group.

CTRL=control; ABA=activity-based anorexia

Table 1. Conditions of the primary and secondary antibodies used in WB analysis.

Protein	Primary antibody	Secondary antibody	ECL Substrates
GluA1 (108 kDa) (RRID: AB_641040; Cell Signaling)	1:2000 iblock buffer O/N 4°C	1:1000 iBlock 1 hr RT anti-Rabbit IgG HRP (RRID: AB_2099233; Cell Signaling)	WESTAR ANTARES (Cyanagen)
GluA2 (108 kDa) (RRID: AB_10622024; Cell Signaling)	1:1000 iblock buffer O/N 4°C	1:1000 iBlock 1 hr RT anti-Rabbit IgG HRP (RRID: AB_2099233; Cell Signaling)	WESTAR ANTARES (Cyanagen)
GluN1 (120 kDa) (RRID: AB_1904067; Cell Signaling)	1:1000 iblock buffer O/N 4°C	1:1000 iBlock 1 hr RT anti-Rabbit IgG HRP (RRID: AB_2099233; Cell Signaling)	WESTAR NOVA 2.0 (Cyanagen)
GluN2A (180 kDa) (RRID: AB_2112295; Cell Signaling)	1:1000 iblock buffer O/N 4°C	1:1000 iBlock 1 hr RT anti-Rabbit IgG HRP (RRID: AB_2099233; Cell Signaling)	WESTAR ANTARES (Cyanagen)
GluN2B (180 kDa) (RRID: AB_2798506; Cell Signaling)	1:1000 iblock buffer O/N 4°C	1:1000 iBlock 1 hr RT anti-Rabbit IgG HRP (RRID: AB_2099233; Cell Signaling)	WESTAR ANTARES (Cyanagen)
SAP97 (97 kDa, observed band 140 kDa) (RRID: AB_2091910; Cell Signaling)	1:1000 iblock buffer O/N 4°C	1:2000 iBlock 1 hr RT anti-Rabbit IgG HRP (RRID: AB_2099233; Cell Signaling)	WESTAR NOVA 2.0 (Cyanagen)
SAP102 (102 kDa) (RRID: AB_2799325; Cell Signaling)	1:1000 iblock buffer O/N 4°C	1:2000 iBlock 1 hr RT anti-Rabbit IgG HRP (RRID: AB_2099233; Cell Signaling)	WESTAR NOVA 2.0 (Cyanagen)
PSD95 (95 kDa) (RRID: AB_561221; Cell Signaling)	1:4000 iblock buffer O/N 4°C	1:2000 iBlock 1 hr RT anti-Rabbit IgG HRP (RRID: AB_2099233; Cell Signaling)	Westar SUN (Cyanagen)
Neuroligin-1(94 kDa) (RRID: AB_2151646; Synaptic System)	1:1000 iblock buffer O/N 4°C	1:2000 iBlock 1 hr RT anti-Rabbit IgG HRP (RRID: AB_2099233; Cell Signaling)	WESTAR NOVA 2.0 (Cyanagen)
N-Cadherin (100 kDa) (RRID: AB_2687616; Santa Cruz)	1:2000 iblock buffer O/N 4°C	1:2000 iBlock 1 hr RT anti-Mouse IgG HRP (RRID: AB_258167; Sigma)	WESTAR NOVA 2.0 (Cyanagen)
F-actin (42 kDa) (RRID: AB_302794; Abcam)	1:1000 iblock buffer O/N 4°C	1:1000 iBlock 1 hr RT anti-Mouse IgG HRP (RRID: AB_258167; Sigma)	WESTAR NOVA 2.0 (Cyanagen)
α - tubulin (50 kDa) (RRID: AB_477593; Sigma)	1:20.000 iblock buffer O/N 4°C	1:15.000 iBlock 1 hr RT anti-Mouse IgG HRP (RRID: AB_258167; Sigma)	Westar SUN (Cyanagen)

Table 2. Effects of ABA induction on the average spines length and head width, expressed as μm±SEM, of the mushroom-, stubby-, thin-shaped spines in the mPFC measured in the acute phase of the pathology (PND42) and after a 7-days recovery period (PND49).

* $p<0.05$, ** $p<0.01$ vs. CTRL-acute phase; #$p<0.05$ vs ABA-recovery (two-way ANOVA followed by Bonferroni's multiple comparisons test).

		Acute phase (PND 42)		After recovery (PND49)		Two-way ANOVA manipulation x time of sacrifice interaction
		CTRL	ABA	CTRL	ABA	
Mushroom	**length**	1,4950 ± 0,1003	1,7475± 0,0404*	1,7176± 0,0265	1,2517± 0,0445	$F_{(1,28)}=10.31$, p=0.003
	width	0,7232± 0,0719	0,4862± 0,0435**	0,6222± 0,0336	0,4430± 0,0271	$F_{(1,27)}= 5.734$, p=0.0238
Stubby	**length**	0,6700± 0,0196	0,7119± 0,0236	0,7932± 0,0315	0,5320± 0,0166	$F_{(1,28)}=3.830$, p=0.0604
	width	0,4028± 0,0318	0,2831± 0,0184*	0,4342± 0,0280	0,2981± 0,0198#	$F_{(1,28)}= 6.214$, p=0.0189
Thin	**length**	1,3185± 0,0757	1,4016± 0,0788	1,4674± 0,0826	1,1081± 0,0799	$F_{(1,28)}=1.644$, p=0.2103
	width	0,5868± 0,0414	0,4012± 0,0477*	0,5648± 0,0467	0,4421± 0,0478	$F_{(1,28)}= 5.060$, p=0.0325

Figure 1

JNC_15605_Fig-1.jpg
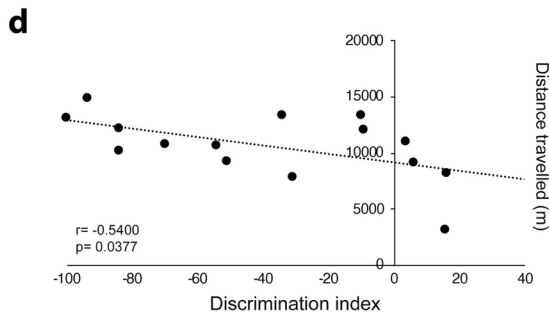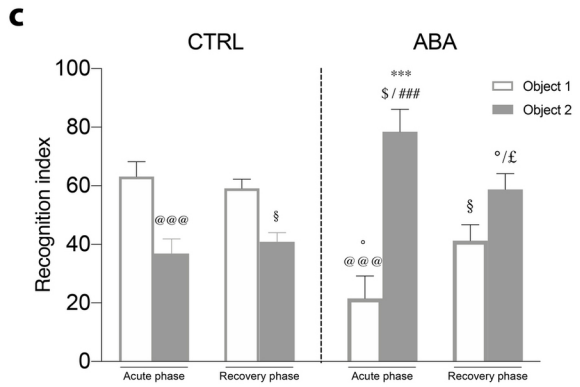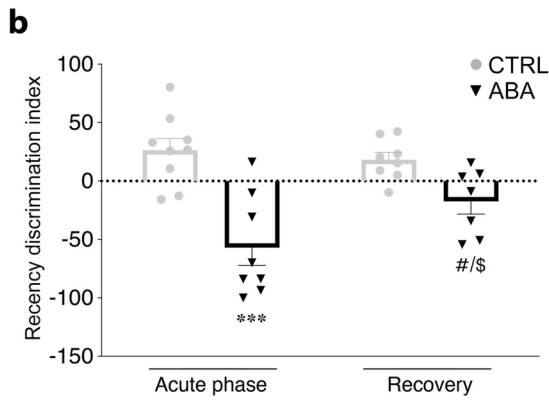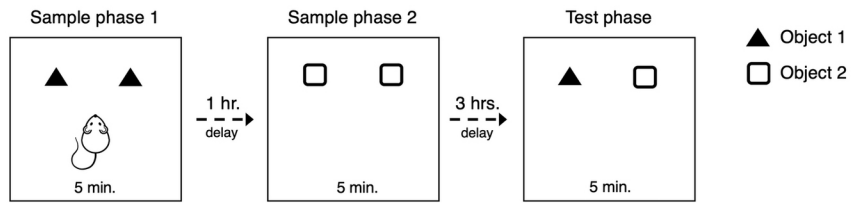
Figure 2
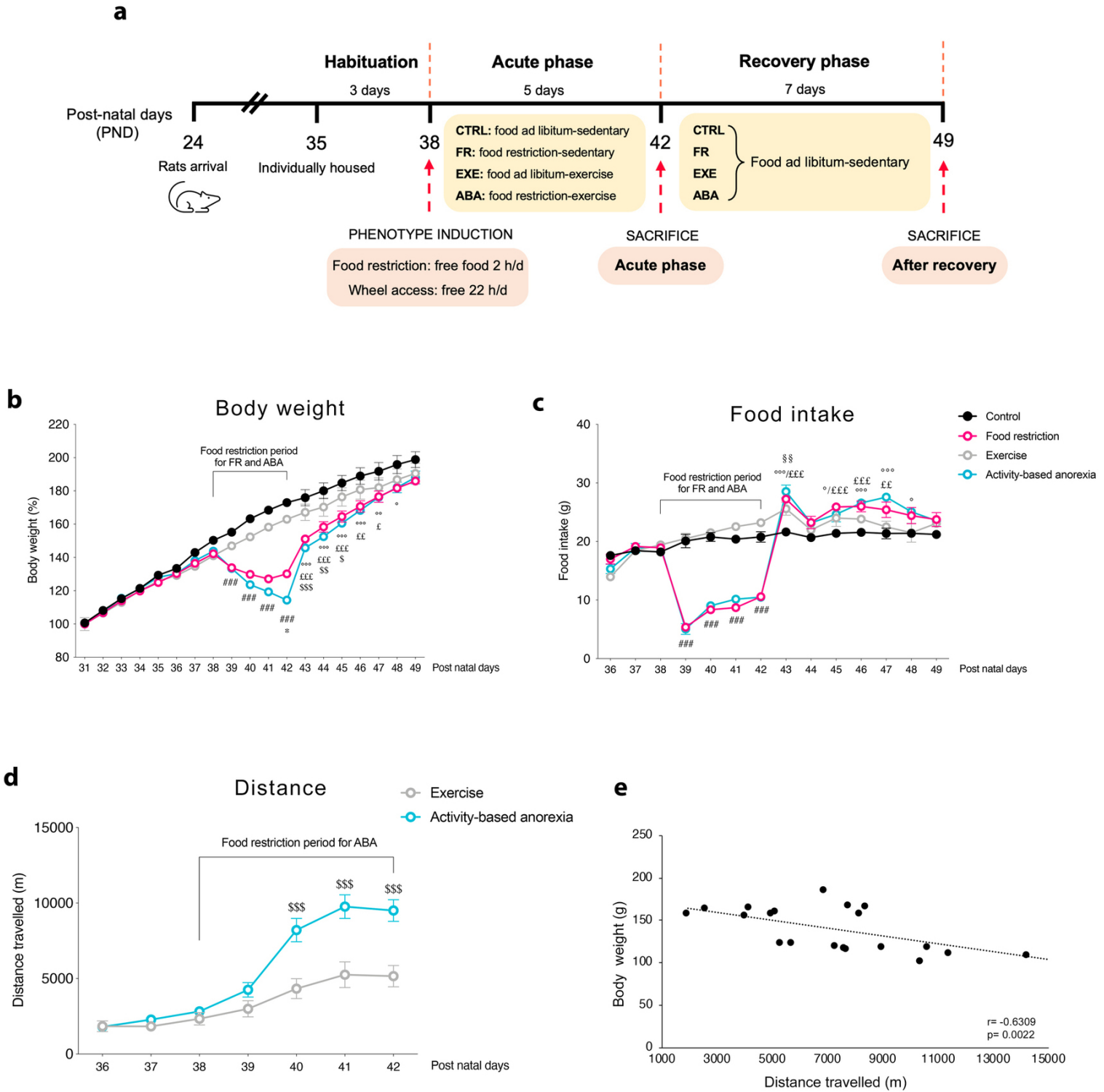
Figure 3
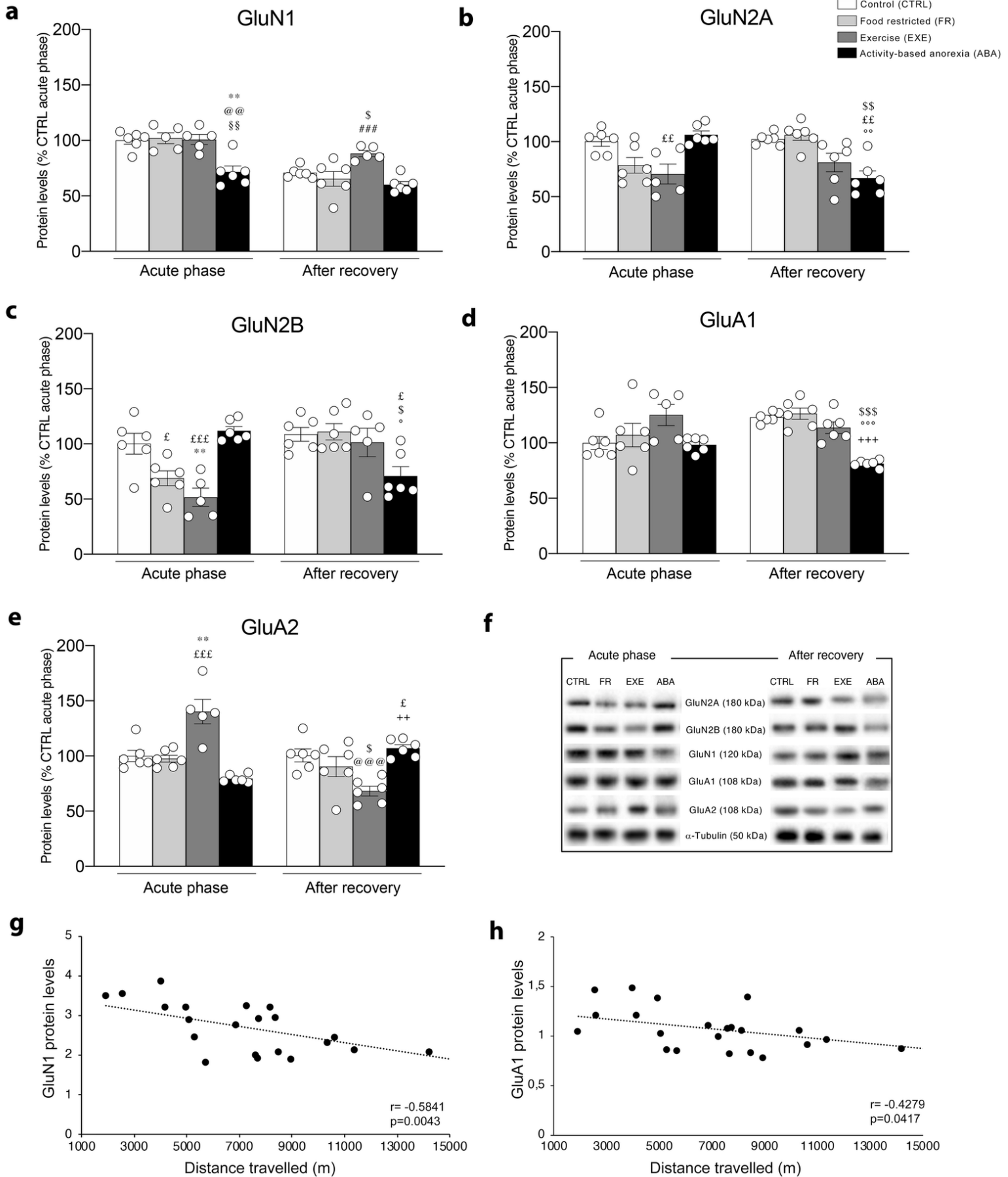
JNC_15605_Figure 3.tif
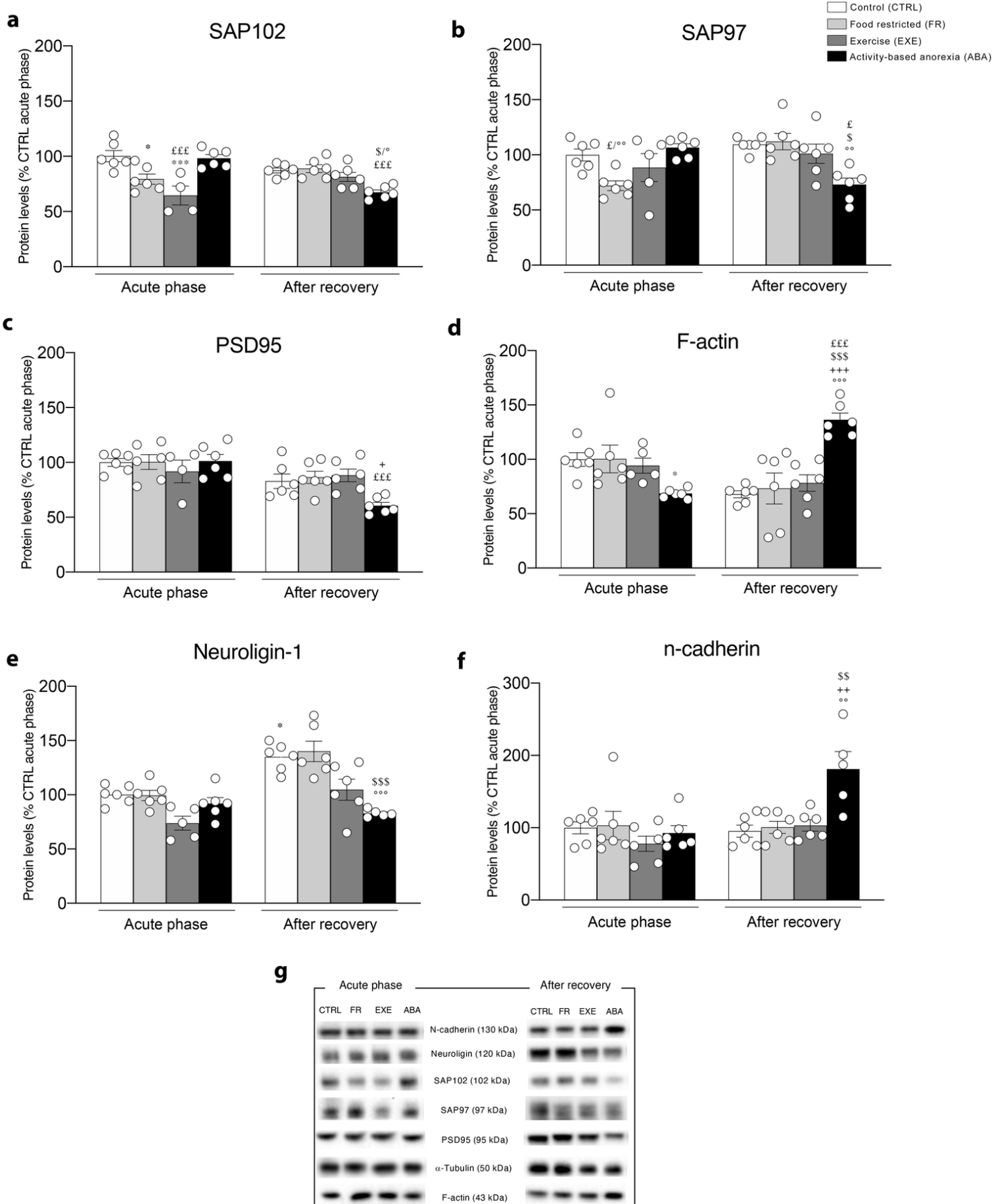
Figure 4
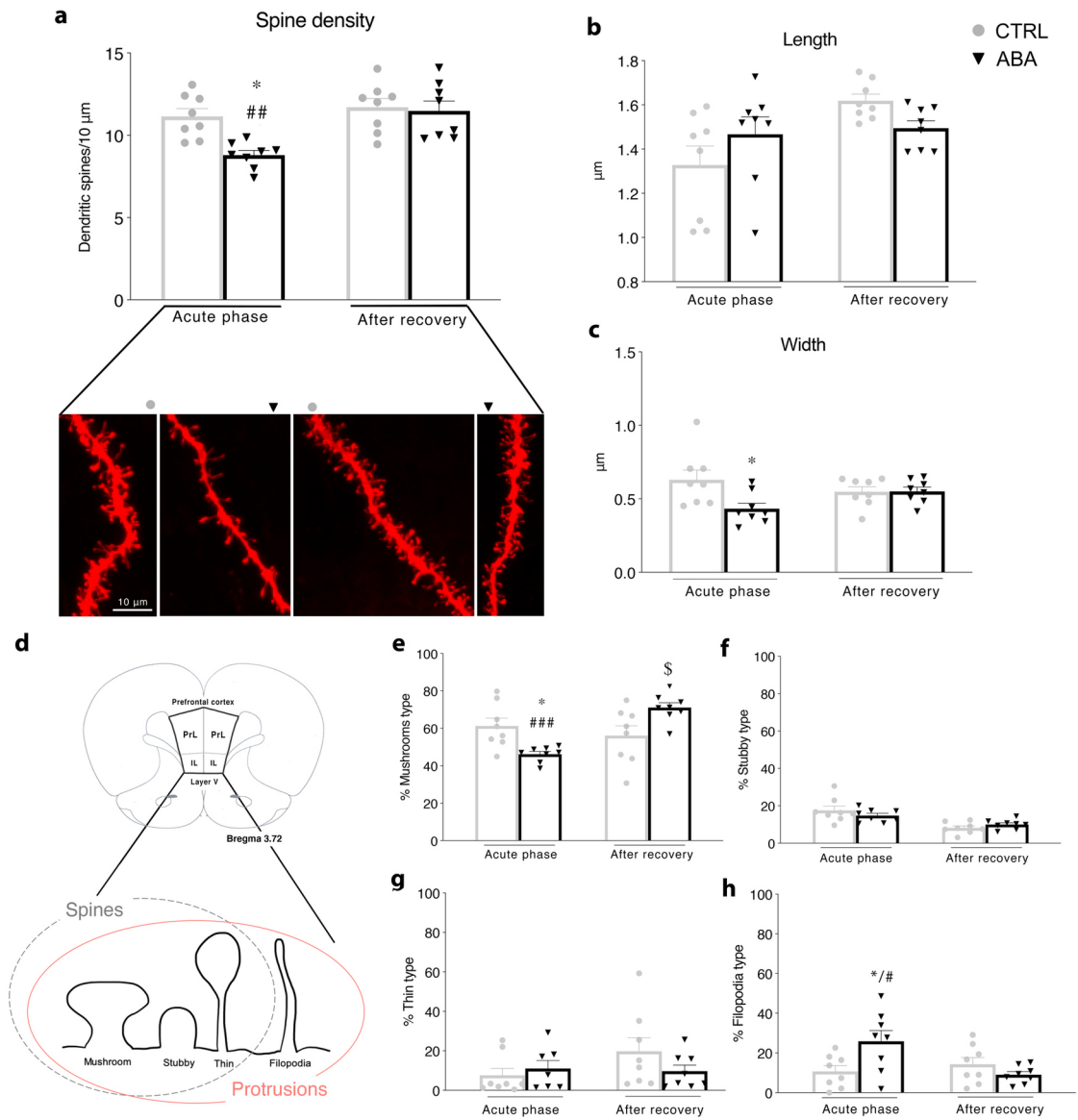
JNC_15605_Fig-4.jpg

a   Temporal order object recognition test

b

c

d

r= -0.5400
p= 0.0377

e

r= 0.5068
p= 0.0031

JNC_15605_Fig-5.jpg